Physics in Medicine & Biology

PAPER

A handheld SPIO-based sentinel lymph node mapping device using differential magnetometry

To cite this article: S Waanders *et al* 2016 *Phys. Med. Biol.* **61** 8120

IOP Publishing | Institute of Physics and Engineering in Medicine Physics in Medicine & Biology

Phys. Med. Biol. **61** (2016) 8120–8134 doi:10.1088/0031-9155/61/22/8120

A handheld SPIO-based sentinel lymph node mapping device using differential magnetometry

S Waanders, M Visscher, R R Wildeboer, T O B Oderkerk, H J G Krooshoop and B ten Haken

MIRA Institute for Biomedical Technology and Technical Medicine, University of Twente, The Netherlands

E-mail: s.waanders@utwente.nl

Received 11 April 2016, revised 12 September 2016
Accepted for publication 4 October 2016
Published 26 October 2016

Abstract

Sentinel lymph node biopsy has become a staple tool in the diagnosis of breast cancer. By replacing the morbidity-plagued axillary node clearance with removing only those nodes most likely to contain metastases, it has greatly improved the quality of life of many breast cancer patients. However, due to the use of ionizing radiation emitted by the technetium-based tracer material, the current sentinel lymph node biopsy has serious drawbacks. Most urgently, the reliance on radioisotopes limits the application of this procedure to small parts of the developed world, and it imposes restrictions on patient planning and hospital logistics. Magnetic alternatives have been tested in recent years, but all have their own drawbacks, mostly related to interference from metallic instruments and electromagnetic noise coming from the human body. In this paper, we demonstrate an alternative approach that utilizes the unique nonlinear magnetic properties of superparamagnetic iron oxide nanoparticles to eliminate the drawbacks of both the traditional gamma-radiation centered approach and the novel magnetic techniques pioneered by others. Contrary to many other nonlinear magnetic approaches however, field amplitudes are limited to 5 mT, which enables handheld operation without additional cooling. We show that excellent mass sensitivity can be obtained without the need for external re-balancing of the probe to negate any influences from the human body. Additionally, we show how this approach can be used to suppress artefacts resulting from the presence of metallic instruments, which are a significant dealbreaker when using conventional magnetometry-based approaches.

Keywords: biomagnetism, sentinel lymph node, magnetometry, nanoparticles, SPIO, superparamagnetism, surgical tools

(Some figures may appear in colour only in the online journal)

1. Introduction

The sentinel lymph node (SLN) procedure is a standard tool to assess the point to which certain cancers have developed (Veronesi *et al* 1996). It is the current standard of care for breast cancer and melanoma in many countries (Schraffordt Koops *et al* 1999). Currently, the procedure is most commonly performed by injecting a combination of a blue dye and a radioactive nanocolloid (^{99m}Tc albumin) near the tumor, after which the lymphatic drainage path is followed by a gamma probe until a lymph node is found (figure 1). By performing histopathology on this lymph node, the nodal status of the entire lymphatic basin draining the tumor area can be determined, potentially sparing the patient a full axillary clearance, which is associated with severe morbidity and complications (Lyman *et al* 2014).

Although the combined method works well, the use of the radioactive tracer has drawbacks, including a significant logistical burden on the hospital, which limits its use in third world countries and other regions without ready access to radioisotopes (Ahmed *et al* 2014). However, a key effort is underway to develop a magnetic alternative to the previously mentioned radioactive method (Douek *et al* 2014, Thill *et al* 2014, Piñero-Madrona *et al* 2015), but this approach is limited by inductively coupled noise stemming from the diamagnetism of the human body, which creates a constant need to balance the instrument intra-operatively (Visscher *et al* 2014). We believe that by specifically searching for the nonlinear magnetic signature of the magnetic tracer used (for example, Resovist^{TM}, Bayer Schering Pharma GmbH), we can improve the selectivity and sensitivity of such a magnetometer setup and thus increase its clinical applicability. Additionally, conventional magnetometry-based techniques are hampered by the presence of metallic objects like surgical instruments, as they induce noise into the instruments, rendering them useless. Our demonstrated approach negates these noise sources, and enables effortless integration of the technique into standard clinical practice.

Superparamagnetic iron oxide nanoparticles (SPIONs) have been implemented in various medical and biological applications (Krishnan 2010), frequently as a tracer material or contrast agent, with a variety of different techniques employed for their detection. Examples of these techniques include magnetic particle imaging (MPI) (Gleich and Weizenecker 2005), magnetic resonance imaging (MRI) (Pankhurst *et al* 2003), frequency mixing (Krause *et al* 2007, Nikitin *et al* 2008), magnetorelaxometry (MRX) (Knopke *et al* 2013, Liebl *et al* 2014, De Haro *et al* 2015) and AC susceptibility measurements (Kuipers *et al* 2008, Quini *et al* 2015). Of these techniques, we can broadly distinguish those relying on the strong susceptibility of the tracer material (MRX, AC susceptibility, MRI) and those utilizing the nonlinear magnetic characteristics of the material (MPI, frequency mixing). Differential magnetometry, the focus of this paper, falls into the latter category. However, many these applications and techniques are capital intensive and cumbersome, limiting their use in the operating theatre due to stringent requirements with regard to, for example, background magnetic fields. Still, the unique magnetic signature of these particles opens up a world of opportunities in diagnostics, and we aim to bring such a system using nanoparticles into the operating theatre.

This article describes the development of a handheld magnetic nanoparticle detector suitable for intra-operative use. It is specifically aimed at exploiting the nonlinear magnetic properties of these particles, using a measurement sequence we introduced as *differential*

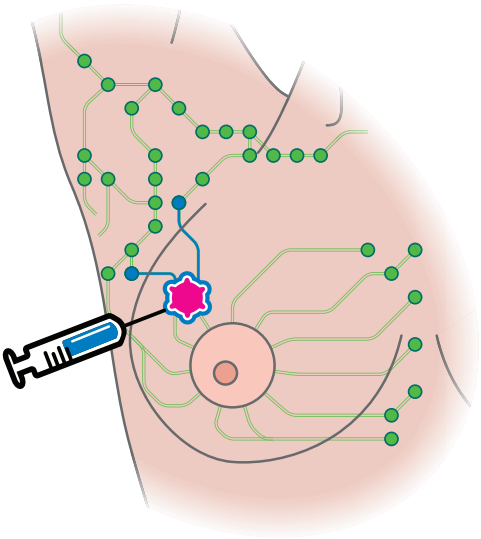

Figure 1. Schematic representation of the sentinel lymph node localization procedure, showing the peritumoral injection site, and tracer travelling to two sentinel lymph nodes.

magnetometry (Visscher *et al* 2014), which is currently patent pending (Waanders *et al* 2012). We describe the development and characteristics of the handheld device and briefly explore possible strategies for improving the system's resolution and other performance figures.

1.1. Clinical requirements

The starting point of any development process for a medical apparatus should be the clinical case at hand, and it is no different here. A few considerations must be made with regards to user friendliness of the device, considering its usage by a medical professional in the operating theatre. For proper adoption of magnetic sensing technology in the operating room, the sensor should be robust against electromagnetic noise coming from other equipment, as well as the tools used by the surgeon during the procedure. With these tools being made primarily out of surgical (carbon) steel, magnetic interference from scalpels, retractors et cetera is a serious problem for conventional alternating current (AC) magnetometry. In that approach, the generated magnetic field is strongly perturbed by these instruments, which leads to erroneous signals from the probe. Additionally, the non-constant magnetic susceptibility of the human body forms another resolution limiter. However, all these unwanted signals have in common that their magnetic behavior in the low field (mT) regime is linear.

Conventional alternating current (AC) magnetometry has proven to be an accurate tool for establishing the magnetic properties of a sample (Kuipers *et al* 2008). A sample is subjected to an alternating magnetic field, which results in an alternating magnetization of the sample. It is then, via Faraday's principle of induction, detected by a sensitive search coil, usually placed coaxially with the excitation coil. The resultant measurement is of the net magnetic susceptibility of the total sample volume probed by the detection coil. However, this leads to the limitations of a conventional ac magnetometer with regards to intra-operative detection.

Consider a tissue sample in which SPIO nanoparticles are placed. These particles, with a large (superpara)magnetic moment, usually dominate the measured signal for moderate amounts of SPIONs, as their magnetic susceptibility χ_0 is roughly seven orders of magnitude higher than that of the surrounding diamagnetic tissue. However, as the particle concentration reduces, so does the part of the signal originating from the nanoparticles, which at some point becomes of the same order of magnitude as the signal from the diamagnetic tissue. At this point, it becomes hard to localize the particles because of the low signal to noise ratio (SNR). This means that the maximum attainable sensitivity of such a probe is not limited by the hardware or noise performance of the probe itself, but rather by the tissue under investigation, which is a limitation that cannot be alleviated without obtaining a specific contrast between the SPIONs and the tissue sample (Visscher *et al* 2015).

From animal studies (Anninga *et al* 2013, Pouw *et al* 2015) performed with AC magnetometers, we know that for ferucarbotran tracers, as little as 10 μg iron (Fe) of tracer material ends up in the clinically relevant sentinel lymph nodes, and that they are located up to four centimeters deep in the body. Because the nodes are found intraoperatively, this depth requirement is not as strict as that, but still we aim for a mass resolution of our system of 5 μg Fe directly underneath the probe to accurately assess all localized nodes for the presence of SPIONs.

Additional requirements stem from the geometry of the surgical procedure. Many procedures nowadays are executed in the least invasive way possible, meaning that any probe which is to be inserted into the surgical cavity should be as thin as possible to minimize obstruction of the surgeon's field of view. Our probe is designed with a 20 mm outside diameter to accomodate this, similar to the outside diameter of clinically applied gamma probes.

2. Differential magnetometry

Superparamagnetic iron oxide nanoparticles have been extensively studied as contrast materials in magnetic resonance imaging, and are slowly making their way into other medical applications. Within the class of SPIONs, much research has focused on the MRI contrast agent Resovist, although many others have been produced, with varying clinical and commercial success (Pankhurst *et al* 2003). Because it is one of the few materials available and approved for clinical use, it was chosen as tracer material for this research. These particles consist of a 6–10 nm sized iron oxide core, encapsulated in a coating of biocompatible material, such as (carboxy)dextran. The use of these particles in magnetic resonance imaging and standard magnetometry is based on the strong magnetic susceptibility χ when exposed to an external magnetic field. However, as explained in the previous section, as the amount of contrast agent decreases, this magnetic signature becomes obfuscated by the diamagnetic signal contribution of the surrounding tissue. To reliably detect small amounts of particles in a big volume containing other materials, one should obtain a signal which is specific to the particles, much like the radiation signature of the ^{99m}Tc albumin colloid used in the radioactive method.

This specific signature can be found in the strongly nonlinear magnetization characteristics of the SPIO nanoparticles, which contrasts with the linear magnetization curve of tissue, which is mostly diamagnetic. By exposing the sample under investigation to a sequence of varying and static magnetic fields, we specifically target the SPIO nanoparticles and are thus able to localize them in tissue.

The magnetization of a single SPIO nanoparticle is governed (in the simplest approximation) by the so-called Langevin equation:

$$M = M_s \mathcal{L}(x) \qquad \mathcal{L}(x) = \coth x - \frac{1}{x} \tag{1}$$

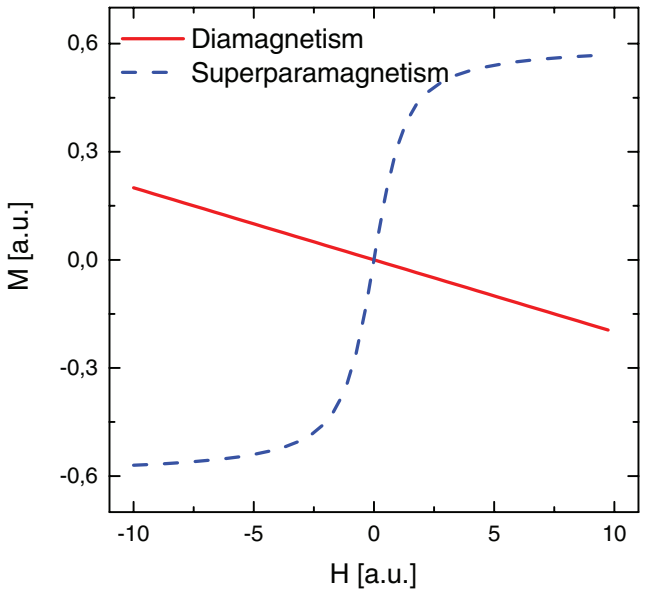

Figure 2. Magnetization versus applied field for an ideal SPIO nanoparticle (blue) and a diamagnetic material (red).

where x represents the ratio between magnetic and thermal energy: $x = \frac{\mu_0 mH}{k_B T}$.

As can be seen in figure 2, this leads to a strongly nonlinear magnetization curve, which saturates for high applied fields, where all magnetic moments within the particle ensemble are aligned and the magnetization of the particle can no longer increase.

When a sample containing superparamagnetic iron oxide nanoparticles is exposed to a small oscillating magnetic field H_{ac}:

$$H_{ac} = S_{exc}\frac{I_{ac}\sin\omega t}{\mu_0}, \tag{2}$$

where S_{exc} is the coil constant of the excitation coil in [T/A], I_{ac} the excitation current and ω the oscillation frequency, this will result in an oscillating magnetization, which is picked up as a voltage over the detection coil.

This is the basis of conventional magnetometry, in which the detection voltage scales with the *derivative* of the magnetization curve around zero, or the *magnetic susceptibility* χ. However, diamagnetic contributions from the tissue surrounding the nanoparticles also contribute to this signal, and can, in principle, obscure the signal coming from a small amount of particles.

Differential magnetometry (DiffMag) uses the nonlinearity of the magnetization curve of SPIO nanoparticles, whereas the background signal is linear, even for moderately strong fields (figure 2). Interestingly, in SPIONs similar to Resovist, this nonlinearity is already strongly present at low fields in the order of 1 mT, which allows for a low-power solution, ideal for intraoperative use with simple hardware. It should be noted however that the exact shape of the magnetization curve and thus the scale at which nonlinearities occur is strongly dependent on the nanoparticle system. By applying a series of alternating offset fields with amplitude H_{dc} to the sample while probing the derivative of the magnetization curve $\frac{dM}{dH}$, we can compare the

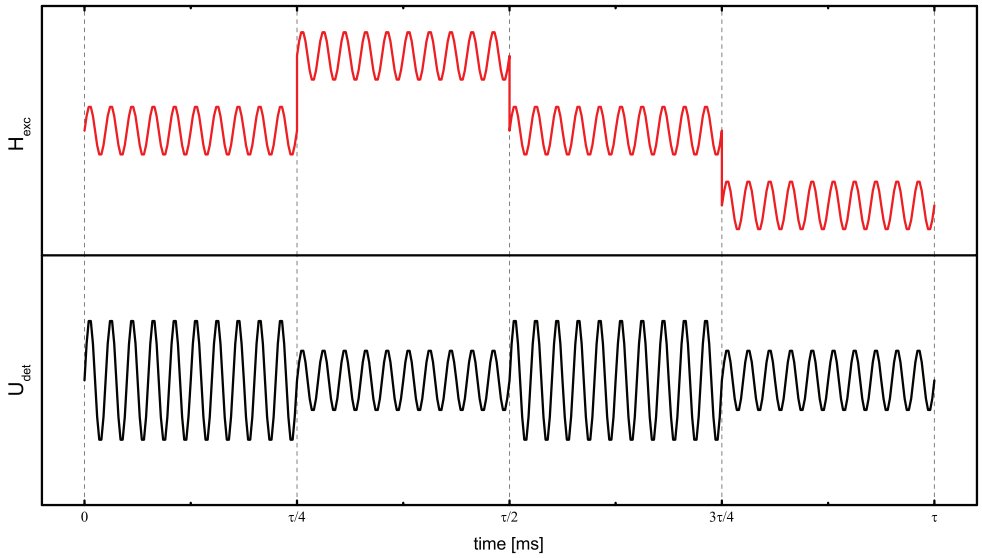

Figure 3. DiffMag modulated excitation field (top), resultant detector voltage (bottom). Figure not to scale.

value of this derivative at various points on the curve, enabling us to distinguish between linearly magnetic tissue and superparamagnetic particles. The resulting field sequence is shown in figure 3.

Mathematically, the DC excitation pulse is defined as

$$H_{\mathrm{dc}} = h_{\mathrm{dc}}\Gamma(t) \tag{3}$$

$$\text{with} \quad \Gamma(t) = \begin{cases} 1 & \tau/4 < t < \tau/2 \\ -1 & 3\tau/4 < t < \tau \\ 0 & \text{elsewhere} \end{cases} \tag{4}$$

Here, τ defines the duration of a single, full DiffMag cycle, and h_{dc} the amplitude of the pulse. At the detector, the detected signal amplitude u depends on the amplitude of the alternating sample magnetization M:

$$u = -2\pi f S_{\mathrm{det}}(z) V_c M \tag{5}$$

where f is the excitation field frequency, $S_{\mathrm{det}}(z)$ the coil constant (in T/A) and V_c the magnetic core volume.

The single-cycle DiffMag signal is defined as

$$\begin{aligned} \Delta\bar{u} &= \frac{1}{2}\left[\Delta\bar{u}_+ + \Delta\bar{u}_-\right] \\ &= \frac{1}{2}\left[(\bar{u}_0 - \bar{u}_+) + (\bar{u}_0 - \bar{u}_-)\right] \end{aligned} \tag{6}$$

Here, $\bar{u}_0$ represents the mean voltage in the absence of a pulse, and $\bar{u}_-$ and $\bar{u}_+$ represent the mean sensor voltage during a negative and positive pulse, respectively. The polarity change in the pulse allows for compensation of local field imbalances, for example due to the earth's magnetic field. Earlier, we demonstrated the efficacy of this procedure in a laboratory setting (Visscher *et al* 2014), allowing us to focus on a practical real-world application now. This

procedure results in background-independent detection of SPIO nanoparticles, in which the measured signal scales linearly with the amount of nanoparticles, but drops off with distance, following Ampère's law.

2.1. Noise compensation

Various sources influence the voltage resulting from the detection circuit before calculating the DiffMag signal, many of which are not related to the particles used. Most of these are reliably filtered out by signal reconstruction, but the large inductive load on the coils may cause dynamic range problems, so a compensation strategy was developed to dynamically cancel out unwanted noise contributions.

The inherent differential nature of the DiffMag pulse sequence allows for subtraction of an arbitrary baseline value, as long as this baseline is kept at a constant value throughout one measurement cycle. This allows for electronic compensation of any linear magnetic or electronic influences that would otherwise cause the sensor voltage to drift outside of the dynamic range of the receive chain, which is limited to obtain excellent sensitivity. This sensor drift can be caused by a variety of phenomena, like heating and subsequent thermal expansion of the excitation coil, but also from the presence of stray magnetic fields originating from magnetized surgical tools, for example. This is implemented by means of a compensation coil wound around the detection gradiometer, which couples a small, controlled amount of magnetic flux into the detection coils to cancel any imbalances.

More specifically, the low field regime (1 mT) in which DiffMag operates allows us to filter out the inductive response from surgical steels present near the probe tip. Similar to the linear diamagnetic signal from tissue, surgical steel (nonmagnetic) shows linear magnetic behavior in low field regimes, due to the fact that its saturation magnetization is orders of magnitude higher than that of the SPIONs. This means that under DiffMag excitation parameters, the inductive behavior from the surgical tools does not vary with the strength of the excitation pulse, meaning it is filtered out by the subtraction operation in equation (6).

Mainly though, noise is suppressed by isolation of the main frequency through a process known as *synchronous detection*, where the orthogonality of sines is exploited. Using the excitation signal as a reference, the detected signal is multiplied with the reference. This yields a signal U_{psd} containing the sum and difference frequency components from signal and reference (equation (9)).

$$U_{\mathrm{det}} = u_{\mathrm{det}} \sin(2\pi f t + \phi_{\mathrm{det}}) \tag{7}$$

$$U_{\mathrm{ref}} = \sin(2\pi f t + \phi_{\mathrm{ref}}) \tag{8}$$

$$U_{\mathrm{psd}} = \frac{1}{2} u_{\mathrm{det}} \left[\cos(\phi_{\mathrm{ref}} - \phi_{\mathrm{det}}) - \cos(4\pi f t + \phi_{\mathrm{ref}} + \phi_{\mathrm{det}})\right] \tag{9}$$

In the special case where the signal frequency is equal to the reference frequency, the DC component of equation (9) is a measure which scales with the desired signal intensity. This DC signal is isolated by low-pass filtering of the multiplied signal.

This allows us to recover the original measured signal, without noise:

$$u_{\mathrm{det}} = \sqrt{X^2 + Y^2} \qquad \text{and} \qquad \phi_{\mathrm{det}} = \tan^{-1}\left(\frac{Y}{X}\right) \tag{10}$$

$$\text{with} \qquad X = u_{\mathrm{det}} \cos(\phi_{\mathrm{det}}) \quad \text{and} \quad Y = u_{\mathrm{det}} \sin(\phi_{\mathrm{det}}) \tag{11}$$

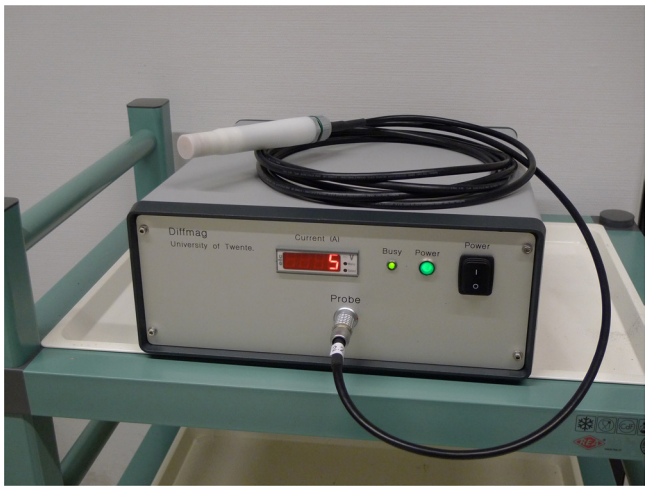

Figure 4. Handheld DiffMag prototype.

3. Experimental setup

The DiffMag handheld system is comprised of three parts: the probe itself, the base unit and a PC which performs all the signal analyses. In the following sections we describe the system in detail.

3.1. Probe design and implementation

To assess the feasibility of the concept introduced in the previous section, a prototype was constructed consisting of an excitation coil surrounded by a detection coil pair which generates the field sequence magnetizing the SPIO nanoparticles. To cancel out the mutual inductance between the detection coil and the excitation coils, the excitation coil pair are placed in series with their polarities reversed, acting as a gradiometer. This first-order compensation minimizes the influence of the excitation signal on the detector. The excitation coils are wound with litz wire (Rupalit HF Litze V155, 27×0.071 mm $+ 2 \times 52$) to minimize AC losses. A small compensation coil pair is wound around the detection coils to allow for dynamic field compensation and imbalance correction. All coils were wet wound in epoxy resin (Stycast 1266) to prevent wire movement due to thermal or mechanical stress. The coils are wound on a body composed of a aluminumnitride-boronnitride composite (SHAPAL^{TM} Hi-M soft, Ceratec Technical Ceramics BV, The Netherlands), mainly because of its excellent thermal conductivity and low thermal expansion coefficient. To accomodate for the high hygiene requirements posed by the medical environment in which the probe will operate, the entire probe assembly is placed inside a delrin enclosure for easy cleaning and aestethics. Figure 4 shows the assembled prototype device and its base unit, and figure 5 gives a high-level overview of the system electronics.

The probe body additionally contains a first filter stage (bandpass with 3 dB points at 1 kHz and 15 kHz) which acts as a decoupler between the connecting cable and the coil setup. The coil is driven by a purpose-built current driven amplifier (ServoWatt, 24 V 2 A continuous, 4 A peak output), connected by a shielded cable. The excitation signal is monitored through a shunt resistor in the power amplifier and fed back into the data processing unit to serve as a reference for phase-sensitive signal processing.

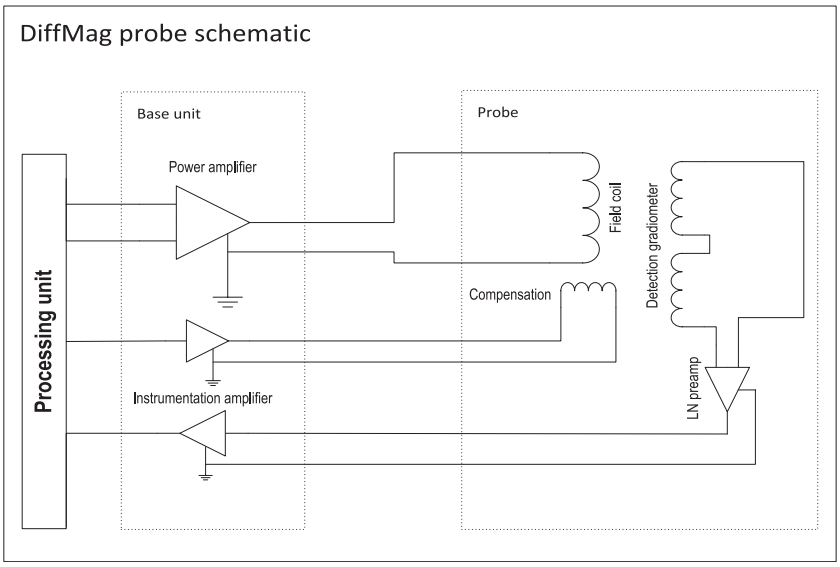

Figure 5. System level electronics description.

4. Results

4.1. Probe characteristics

4.1.1. Tracer sensitivity. The main characteristics of the handheld probe are of course its attainable mass sensitivity, its penetration depth and the lateral sensitivity of the device. A higher sensitivity means that even nodes with the tiniest amounts of SPIONs can be found reliably, whereas an increased penetration depth means that it is easier to localize deeper lying nodes. Finally, a high lateral sensitivity (i.e. a spatially selective probe) is required to distinguish between multiple closely located nodes. Figure 6 shows the measured dose-response curve for the handheld DiffMag probe and a set of artificial lymph nodes containing varying concentrations of Resovist. A calibration set of artificial lymph nodes was produced. To this end, non-magnetic polyvinylchloride (PVC) beads of $r \approx 2.9$ mm and $r \approx 3.6$ mm were filled with, respectively, 30 μL and 60 μL of Resovist dilutions ranging from 5 μg to 1 mg Fe mass and sealed with cyclohexanone. Samples were measured three times to assess reproducibility. Four samples were omitted due to obvious leakage of the container. Samples up to 5 μgFe can reliably be detected above the noise threshold. Samples were placed 1 mm from the tip of the probe, with the total distance between sample and the first detection coil amounting to 2 mm due to the 1 mm probe casing. A small error in the iron concentration (especially in the low concentration samples) occurred because of the cyclohexanone sealing procedure of the pvc beads, which leads to apparently noisy results in the dose-response curve. Measurement results were stable over all three measurements, supporting this hypothesis.

4.1.2. Spatial sensitivity. For reliable operation of the probe during surgery, the probe needs to have a high spatial sensitivity, i.e. the probe's axial full width at half maximum (FWHM) needs to be small. The lateral sensitivity is shown in figure 7. Here, we see that the FWHM is 25 mm, which is strongly influenced by the fact that our phantom lymph node containing the SPIO tracer has a width of 5 mm. This could be improved by decreasing the probe diameter, which comes at the cost of strongly reduced penetration depth.

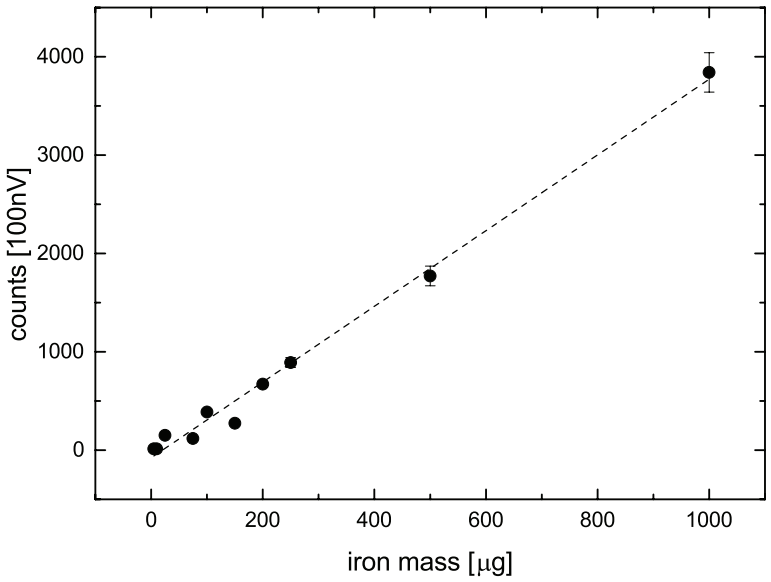

Figure 6. Dose-response curve for Resovist nanoparticles with the DiffMag handheld probe operated at 2.5kHz AC.

4.1.3. Penetration depth. Furthermore, the penetration depth of the probe determines the depth at which a sample of magnetic nanoparticles can be located. Due to the fact that our probe is a simple gradiometer configuration, the penetration depth is of the order of the probe's diameter. The result of this measurement is shown in figure 8. As can be seen here, a sample of 500 μgFe can be measured up to 1.0cm depth. This is sufficient for intraoperative use, but it rules out the possibility of transcutaneous detection of deeply located sentinel lymph nodes prior to incision. If transcutaneous detection is required, a different sensor geometry is required. For example, one could separate excitation and detection coils, and use the dynamic compensation of DiffMag to dynamically decouple the mutual inductances between these two, which would allow for a large excitation coil to increase the probe's penetration depth.

4.2. Excitation optimization

The DiffMag excitation sequence gives the operator a number of parameters which influence the total signal strength obtained from a measurement for a certain type of particle. These are strongly dependent on the dynamical behavior of the particle which is used. Mainly, we are concerned with the frequency of the alternating field, f_{ac}, its amplitude (H_{ac}) and the amplitude of the pulse field (H_{dc}). It is common practice for an alternating field magnetometer to increase the driving frequency of the system, as the detector voltage scales with the frequency of the resultant alternating magnetization. However, because the dynamical behavior of the SPIO tracer depends strongly on both the Brownian and Neel relaxation constants, we find an optimum frequency of 2.5kHz. If the frequency is further increased, the particle signal decays because of lagging Brownian relaxation behavior.

Then, the two parameters that need optimization next are the alternating and offset field amplitudes. These are limited not by the physics of the particle dynamics, but rather by the heat dissipation of the probe itself. As it is a compact handheld instrument, heat production needs to be minimized, and therefore power dissipation is limited. Setting the maximum

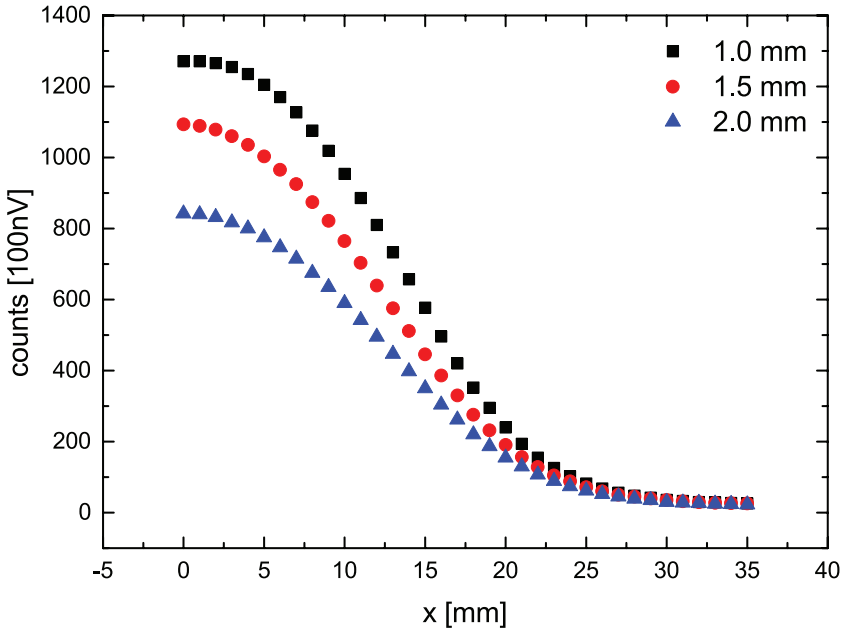

Figure 7. Lateral sensitivity of the DiffMag prototype for a 500 μg Resovist phantom lymph node at 1.0, 1.5 and 2.0 mm from probe tip.

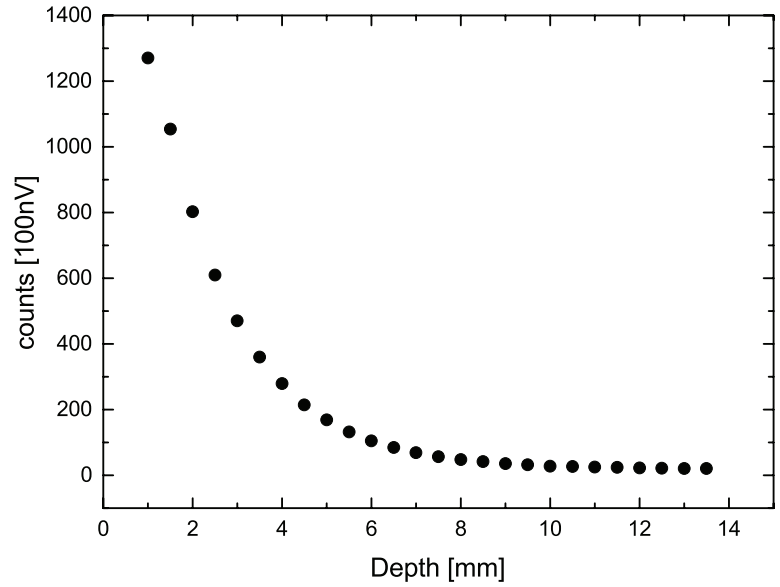

Figure 8. Penetration depth measurement of the DiffMag prototype, measured with a 500 μgFe Resovist phantom lymph node.

heat dissipation to 1W, we can now determine the optimal excitation parameters. As can be deduced from the magnetization curves for our tracers, the alternating magnetization scales linearly with the AC amplitude, but increasing the DC power leads to a higher signal increase because of the strong nonlinearity and the DiffMag principle. Optimal performance of the

probe under constant probe temperature was achieved using an AC amplitude of $I_{ac} = 0.25$ A and and pulse amplitude of $I_{dc} = 1.5$ A using a 30% duty cycle.

Another important limiter for emitter power are the biological limits with regards to specific absorption rate (SAR) and peripheral nerve stimulation (PNS), as described in the ICNIRP guidelines (Ziegelberger 2009). We find that for these excitation parameters, we are still a factor of 10 inside these limits.

4.3. Noise and tissue attenuation

From a clinical point of view, the main prohibiting factor for using sensitive magnetometers during surgery is the presence of surgical instruments, made out of surgical steel, in the vicinity of the probe. The excitation field generates eddy currents inside these materials which couple a huge inductive load into the detection coils, which leads to overloading of the signal processing units, rendering the probe useless in these circumstances. The builtin dynamic compensation in the DiffMag probe detects the (linear) inductive load and generates a cancellation field through the compensation coil pair, negating the effect of the surgical steel. The result of this can be seen in figure 9. Here, we see the signal from a 200 μg Fe Resovist sample next to that of a human hand and surgical steel retractor instrument held next to the sample. We operate the probe in both AC magnetometry and DiffMag mode at constant AC amplitude and frequency, and compare the results. In AC mode, we measure a huge signal from the retractor, which completely obfuscates the SPIO signal. When operating in DiffMag mode, the signal from the retractor is significantly reduced, and the SPIO sample clearly stands out. Also noticable is the slightly negative signal from the human hand in AC mode, and the strong attenuation of this diamagnetic signal in DiffMag mode.

An additional cause of problems in conventional magnetometers is signal drift due to thermal stress. The heat dissipation of the excitation coil causes a change in the mutual induction between the coils because of thermal expansion, which leads to an increasing imbalance of the gradiometer. This results in a drifting output voltage. Because of the differential nature of DiffMag, and the fact that the timescale of a single DiffMag sequence (40 ms) is much shorter than the timescale at which thermal drift occurs, we have not observed any drift of the output signal in DiffMag mode.

Because of the excellent attenuation of external noise, both inductive and resistive, the noise floor of the device is composed of different noise sources inside the electronics of the probe itself. The main cause of noise is thermal or Johnson noise in the resistive components of the setup and the power amplifier and the quality of the data acquisition system. The total noise figure of the sensor was measured to be 12 $\mathrm{nV}/\sqrt{\mathrm{Hz}}$.

5. Discussion

In this paper, we have shown that selective detection of magnetic nanoparticles in a diamagnetic environment is feasible, and can be implementated in a compact, low power, handheld device. However, some points for improvement are still standing, mostly related to the penetration depth of the probe (i.e. the depth at which SPIO-positive nodes can be detected), and the dynamic compensation. Here, we address both points and compare the demonstrated approach to currently employed techniques. In terms of experimental details, the pvc beads used as artifical lymph nodes did not suffice as reliable sample containers, with many problems concerning leakage and measurement accuracy occured here. We suggest placing samples in small Eppendorf tubes for measurements requiring high spatial and quantitative accuracy.

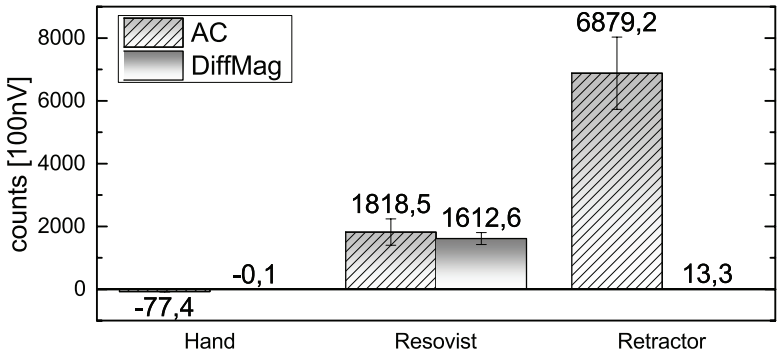

Figure 9. Signal counts for a 200 μg Fe Resovist tracer, a human hand and a surgical steel retractor, in AC mode (left) and DiffMag mode (right).

5.1. Penetration depth

From literature it is known that in the case of breast cancer, sentinel lymph nodes are found at an average depth from the skin of 4.5 cm. Combined with the lowest concentration of SPIONs observed in trials (10 μg Fe), this leads to a stringent resolution requirement, which is currently unmatched by both conventional magnetometry and differential magnetometry. This low penetration depth is primarily governed by the small probe diameter, which dominates the field penetration in Ampère's law, if one assumes a constant baseline noise. Larger coils will obviously show higher baseline noise due to higher coil inductance and resistance, which in turn stresses the entire excitation and detection chain. In an earlier article, we have shown that for a conventional magnetometer, simply increasing the probe diameter does not actually increase sensing depth, as the amount of tissue probed increases as well (Visscher *et al* 2015). For DiffMag, this limitation is nonexistent, and therefore increasing the probe diameter offers a straightforward approach to measuring the presence of SPIO-positive lymph nodes transcutaneously, if measures are taking to limit baseline noise increase. This can be done by adding a second, larger probe to the setup to measure the transcutaneous hotspot, and using the smaller diameter probe intra-operatively.

5.2. Compensation speed

Currently, the demonstrated artefact suppression relies on fast processing of the induced signal and compensating the inductive effect of metallic artefacts close to the probe by coupling additional flux into the detection coils. The quality of this compensation method is limited by the speed at which dynamically changing effects can be compensated, which is limited due to the slow processing speed of the software. By moving signal processing to a dedicated DSP, dynamic compensation of these distorting effects can be achieved.

5.3. Comparison to existing techniques

When observing the entire field of sentinel lymph node biopsy, we can now distinguish four different techniques currently available to the surgeon. First is the use of blue dye as tracer material, which offers visual localization of the node, but does not allow for quantitative evaluation of nodal status. Yet, it is employed in hospitals where the use of radio-isotopes is impossible, due to inavailability of the tracer or other logistical difficulties. Second, the combined approach which uses blue dye in combination with a technetium nanocolloid. Whilst this method is proven to be very effective and reliable, its reliance on radio-isotopes limits its applicability,

especially in areas of the world without access to nuclear medicine. Third, the conventional magnetometry approach has been tested in various Phase 2 clinical trials, with good results. However, its lack of selective measurements and limited penetration depth, without the possibility of significant improvements in the future, lead us to believe that the fourth approach using DiffMag is more viable and will lead to more reliable results, without relying on ionizing radiation and plastic tools. An important point to consider is the tendency towards lower applied doses of contrast agent, which requires higher probe sensitivities. This might have significant advantages in both reduction of MRI artefacts and potential toxicity effects. Clinical evaluation of this instrument is vital to assess its usability, reliability and accuracy in practice.

6. Conclusions

Magnetic sentinel lymph node biopsy is an excellent alternative to conventional radioisotope-based localization methods. Yet it suffers from depth and mass resolution limitations because of the linear magnetization interference from the human body surrounding the SPIO nanoparticles. In this paper, we have shown that differential magnetometry is a feasible alternative to conventional AC magnetometry methods, at much lower field strenghts and power requirements compared to alternative (imaging) technologies. It combines the excellent spatial sensitivity of a handheld search coil with the specificity offered by nonlinear magnetization measurements used by for example magnetic particle imaging and frequency mixing based immunoassays, while keeping energy requirements to a minimum. The latter advantage is a strong plus for working outside shielded rooms and in the operating theatre. We have shown linearity with regards to the amount of tracer present in the nodes, with a detection sensitivity of 5 μgFe and sufficient depth resolution for intra-operative use. Additionally, we show good attenuation of noise caused by the presence of metallic objects close to the probe, by virtue of the relative nature of the DiffMag measurement, which allows us to dynamically compensate for these signals.

Finally, we note that by implementing this selective measure of nanoparticles without background signals from tissue or instrumentarium, this procedure removes the fundamental sensitivity limit that hampers performance of conventional magnetometers in these difficult environments. This also allows for reduction of applied tracer doses with all associated benefits. Clinical evaluation of the probe, preferrably combined with a second, large diameter probe for transcutaneous hotspot measurements is vital to move forward.

Acknowledgments

The authors would like to thank A de Boer, B Vroling, M Koenrades for their contributions to development and testing of the magnetometer and J J Klaase, J Futterer, R Stemerdink, C Joosten and P Meutstege for useful discussions with regards to the usability and requirements for clinical implementation of the handheld magnetometer. Furthermore, the authors thank A Veugelers for creating figure 1.

References

Ahmed M, Purushotham A D and Douek M 2014 Novel techniques for sentinel lymph node biopsy in breast cancer: a systematic review *Lancet Oncol.* **15** e351–62

Anninga B, Ahmed M, Pouw J J, Fratila R M, ten Haken B, Westbroek D, Pinder S E and Douek M 2013 Lymphatic mapping and sentinel lymph node biopsy in an *in vivo* porcine model using a novel magnetic technique *Eur. J. Cancer* **49** S263

De Haro L P *et al* 2015 Magnetic relaxometry as applied to sensitive cancer detection and localization *Biomed. Tech.* **60** 445–55
Douek M *et al* 2014 Sentinel node biopsy using a magnetic tracer versus standard technique: the SentiMAG multicentre trial *Ann. Surg. Oncol.* **21** 1237–45
Gleich B and Weizenecker J 2005 Tomographic imaging using the nonlinear response of magnetic particles *Nature* **435** 1214–7
Knopke C, Wiekhorst F, Eberbeck D, Gemeinhardt I, Ebert M, Schnorr J, Wagner S, Taupitz M and Trahms L 2013 Quantification of magnetic nanoparticle uptake in cells by temperature dependent magnetorelaxometry *IEEE Trans. Magn.* **49** 421–4
Krause H J, Wolters N, Zhang Y, Offenhausser A, Miethe P, Meyer M H F, Hartmann M and Keusgen M 2007 Magnetic particle detection by frequency mixing for immunoassay applications *J. Magn. Magn. Mater.* **311** 436–44
Krishnan K M 2010 Biomedical nanomagnetics: a spin through possibilities in imaging, diagnostics, and therapy *IEEE Trans. Magn.* **46** 2523–58
Kuipers B W M, Bakelaar I A, Klokkenburg M and Erné B H 2008 Complex magnetic susceptibility setup for spectroscopy in the extremely low-frequency range *Rev. Sci. Instrum.* **79** 013901
Liebl M, Steinhoff U, Wiekhorst F, Haueisen J and Trahms L 2014 Quantitative imaging of magnetic nanoparticles by magnetorelaxometry with multiple excitation coils *Phys. Med. Biol.* **59** 6607–20
Lyman G H *et al* 2014 Sentinel lymph node biopsy for patients with early-stage breast cancer: American Society of Clinical Oncology clinical practice guideline update *J. Clin. Oncol.* **32** 1365–83
Nikitin M P, Torno M, Chen H, Rosengart A and Nikitin P I 2008 Quantitative real-time *in vivo* detection of magnetic nanoparticles by their nonlinear magnetization *J. Appl. Phys.* **103** 07A304
Pankhurst Q A, Connolly J, Jones S K and Dobson J 2003 Applications of magnetic nanoparticles in biomedicine *J. Phys. D: Appl. Phys.* **36** 167–81
Piñero-Madrona A, Torró-Richart J A, de León-Carrillo J M, de Castro-Parga G, Navarro-Cecilia J, Domínguez-Cunchillos F, Román-Santamaría J M, Fuster-Diana C and Pardo-García R 2015 Superparamagnetic iron oxide as a tracer for sentinel node biopsy in breast cancer: a comparative non-inferiority study *Eur. J. Surg. Oncol.* **41** 991–7
Pouw J J, Ahmed M, Anninga B, Schuurman K, Pinder S E, Van Hemelrijck M, Pankhurst Q A, Douek M and ten Haken B 2015 Comparison of three magnetic nanoparticle tracers for sentinel lymph node biopsy in an *in vivo* porcine model *Int. J. Nanomed.* **10** 1235–43
Quini C C, Matos J F, Próspero A G, Calabresi M F F, Zufelato N, Bakuzis A F, Baffa O and Miranda J R A 2015 Renal perfusion evaluation by alternating current biosusceptometry of magnetic nanoparticles *J. Magn. Magn. Mater.* **380** 2–6
Schraffordt Koops H, Doting M H E, Vries J D, Tiebosch A T M G, Plukker J T, Hoekstra H J and Piers D A 1999 Sentinel node biopsy as a surgical staging method for solid cancers *Radiother. Oncol.* **51** 1–7
Thill M, Kurylcio A, Welter R, van Haasteren V, Grosse B, Berclaz G, Polkowski W and Hauser N 2014 The Central-European SentiMag study: Sentinel lymph node biopsy with superparamagnetic iron oxide (SPIO) versus radioisotope *Breast* **23** 175–9
Veronesi U *et al* 1996 Sentinel-node biopsy to avoid axillary dissection in breast cancer with clinically negative lymph-nodes *Lancet* **349** 1864–7
Visscher M, Waanders S, Krooshoop H and ten Haken B 2014 Selective detection of magnetic nanoparticles in biomedical applications using differential magnetometry *J. Magn. Magn. Mater.* **365** 31–9
Visscher M, Waanders S, Pouw J and ten Haken B 2015 Depth limitations for *in vivo* magnetic nanoparticle detection with a compact handheld device *J. Magn. Magn. Mater.* **380** 246–50
Waanders S, Visscher M, Oderkerk T, Krooshoop H and ten Haken B 2012 Method and apparatus for measuring an amount of superparamagnetic material in an object *European Patent Application* no. 12194029.0
Ziegelberger G 2009 Statement on the 'Guidelines for limiting exposure to time-varying electric, magnetic, and electromagnetic fields' *ICNIRP Health Phys.* **97** 257–8